

## Finite Element Modeling of Fatigue Crack Growth in Curved-Welded Joints Using Interface Elements

M. S. Alam<sup>1</sup>, and M.A. Wahab<sup>1,2</sup>

**Abstract:** Fatigue life of curved structural joints in ship structures under constant amplitude cyclic loading has been studied in this research. A new approach for the simulation of fatigue crack growth in welded joints has been developed and the concept has been applied to welded curved butt-joints. The phenomena of crack propagation and interface debonding can be regarded as the formation of new surfaces. Thus, it is possible to model these problems by introducing the mechanism of surface formation. In the proposed method, the formation of new surface is represented by interface element based on the interface surface potential energy. The properties of this interface element represent the bonding strength of the material. As the cyclic load continues, the bonding strength decreases between the interacting surfaces and the crack starts to propagate slowly. Based on this concept, an ANSYS input file has been written for the simulation of crack propagation in the curved welded butt-joints. Using this code, the fatigue crack growth rate and fatigue crack propagation life of 3-D FEM (finite element method) models of welded curve butt-joints and 2-D models for T-joints for different stress/load ratios have been analyzed. The variations of crack-opening-displacement (COD) and crack-tip-strain over crack-tip-stress have also been calculated. For the validation of the simulation, experiments have been conducted and generally good agreement has been achieved. The simulation method is relatively simple compared to other conventional FEM method and effective in many applications.

**keyword:** Interface elements, Interface potential, Fatigue crack growth rate, Finite element method, Curved-butt-joint.

### Nomenclature

$a$  half crack length for a central crack  
 $a_f$  final crack length  
 $a_o$  initial crack length  
 $C$  material dependent constant  
 $da/dN$  crack growth rate (crack length per cycle)  
 $E$  modulus of elasticity  
 $f$  load vector  
 $h$  tangent modulus  
 $k$  stiffness matrix  
 $K$  stress intensity factor (MPa $\sqrt{m}$ )  
 $K_{crit}$  critical stress intensity factor (MPa $\sqrt{m}$ )  
 $\Delta K$  range of stress intensity factor  
 $\Delta K_{th}$  range of threshold stress intensity factor  
 $m$  material dependent constant  
 $n$  shape parameter  
 $N$  number of cycles  
 $N_i$  shape function  
 $N_p$  fatigue crack propagation life  
 $R$  stress ratio  
 $r_o$  scale parameter  
 $u_o$  nodal displacement  
 $U_s$  interface energy during crack propagation  
 $W$  potential of external load  
 $w_i$  nodal displacement normal to the surface  
 $\alpha$  a constant  
 $\Pi$  total energy  
 $\delta$  crack opening displacement  
 $\epsilon$  strain  
 $\phi$  surface potential  
 $\gamma$  surface energy per unit area  
 $\eta$  natural coordinate

<sup>1</sup> Department of Mechanical Engineering, Louisiana State University, Baton Rouge, LA 70803, USA

<sup>2</sup> Corresponding author. Tel.:1- 225-578-5823, Fax:1- 225-578-5924, E-mail: wahab@me.lsu.edu

$\sigma$  nominal stress, bonding strength

$\sigma_{cr}$  critical bonding strength

$\sigma_y$  yield stress

$\xi$  natural coordinate

## 1 Introduction

In many structures (ship, railway, aircraft, ship, oil and gas pipelines, off-shore structures etc.) a large number of welded curve-plates and T-fillet joint are used. Fatigue cracks evolved on these joint as a result of repeated cyclic stress. Thus, it is evident that there is a great need for better understanding of the fatigue phenomenon, so that safer structures could be built.

To determine the fatigue life by the Finite Element Method (FEM) the fatigue crack propagation rate with applied load must be calculated. Unfortunately, in traditional FEM the modeling of crack tip propagation with fatigue load is complicated and requires a numerically extensive program. The cracks do not generally propagate with each application of cyclic load. Because materials do not remember load history during cyclic load, the properties of materials are not changed after cyclic load. Therefore, in the traditional methods, the crack tip mesh is redefined or the crack tip node is released in each cycle and the crack-tip extends one element length per cycle when the applied stress reached the maximum level. But in reality, crack advance takes place in very small increments over many cycles. To reduce this limitation, a new approach, the interface element approach is used in this analysis. Basically in crack formation and extension, failure is the consequence of new surface formation accompanied by crack extension. Based on this idea, interface elements (nonlinear element) are used between the crack faces, which explicitly model the formation of new crack surfaces (details are given in the subsequent sections and briefly in [Alam and Wahab (2005)]).

Using this method, the fatigue crack propagation life of welded and weld-repaired joints can be analyzed appropriately. Thus, this research will help to assess the fatigue life and structural integrity of large welded and repair-welded structures (i.e. ship structures, railway, aircraft, oil and gas pipelines and off-shore structures etc.).

## 2 Review of Early Research

Earlier other researchers used numerical approaches for fatigue crack propagation. In this regard, the works of [Newman et al. (1975, 1977, 1988)] and [McClung and Sehitoglu (1989)] are remarkable. A general trend of the numerical approach in this field for the past 25 years can be inferred from [Newman et al. (1975, 1977, 1988), McClung and Sehitoglu (1989)]. Originally, a crack tip node-release scheme was suggested in [Newman (1977)], in which, a change in the boundary condition was characterized for a crack growth. This was achieved by changing the stiffness of the spring elements connected to boundary nodes of a finite element mesh. Before Newman's work, investigators required to change boundary conditions of the crack tip node directly to obtain a free or fixed node. When the crack tip is free, the crack advances by an element length. The approach Newman used to change boundary conditions was to connect two springs to each boundary node [Newman (1977)]. To get a free node, the spring stiffness in terms of modulus of elasticity was set equal to zero, and for the fixed ones it was assigned an extremely large value (about  $10^8$  GPa) which represents a rigid boundary condition. McClung, Sehitoglu and their collaborators have also investigated fatigue crack closure by the finite element method. Their model for the elastic-plastic finite element simulation of fatigue crack growth used a crack closure concept [McClung and Sehitoglu (1989)]. They followed the node-release scheme at the maximum load and the crack tip was extended one element length per cycle. Wu and Elyin (1996) studied fatigue crack closure using an elastic-plastic finite element model. They followed an extension of Newman's node-release scheme. They used a truss element instead of a spring element and released one node after each cycle of fatigue load. Murakawa et al. (1999,2000) and Masakazu et al. (2000) were the first to use the concept of the interface element for the strength analysis of a joint between dissimilar materials. They also used it for the calculation of the strength of peeling of a bonded elastic strip and the fracture strength of a centre cracked plate under static load [Murakawa et al. (2000)]. They further used it for simulation of hot cracking, push-out test of fibers in matrix, ductile tearing and dynamic crack propagation under pulse load and pre-stress condition [Murakawa et al. (1999)]. They have not applied repeated cyclic load for fatigue crack propagation. This is the first study, according to the au-

thors' knowledge, that cyclic loads have been applied to study crack propagation using interface concepts, especially for welded joints.

It should be pointed out that the past use of finite element analyses had certain shortcomings and tremendous improvements have been made in recent versions and have removed many of these limitations. For example, to avoid numerical instability, schemes such as releasing the crack-tip node at the bottom of a loading cycle were adopted in certain studies, for example study conducted by McClung and Sehitoglu [McClung and Sehitoglu (1989)]. They have not considered element bonding stress and surface energy, which are associated with crack formation and crack extension. They also did not consider the changes in material properties during cyclic loads. They applied symmetric boundary conditions at the crack plane and also assumed that the crack can only propagate in symmetric planes. In this study, it is shown that a crack can propagate in both symmetric and anti-symmetric planes about the applied load.

### 3 Mathematical Relation

The crack is formed when the applied stress exceeds the critical bonding strength of the material. The bonding strength decreases with cyclic load and progressively becomes weak. Finally the bond loses its strength and breaks; and cracks form and extend slowly. The total stiffness of the material decreases with the decrease of bonding strength. As the cyclic load continues, the stiffness decreases and the crack propagate slowly. Therefore, there is a close relationship between the bonding strength and crack propagation. To analyze crack propagation under cyclic load, a method using the interface element, which characterizes the element bonding-strength, has been proposed. In this method, the formation and the propagation of the crack are modeled by using the interface element. The mechanical behavior of the interface element is governed by the interface potential,  $\phi$  per unit area of the crack surface. There are wide choices for such a potential [Murakawa et al. (1999), Masakazu et al. (2000)]. In this analysis, the Lennard-Jones type potential  $\phi$  [Masakazu et al. (2000)] is employed because it explicitly involves the surface energy  $\gamma$ , which is necessary to form a new surface. The surface potential per unit of crack surface area  $\phi$  defined by Lennard-Jones is:

$$\phi(\delta) = 2\gamma \left\{ \left( \frac{r_o}{r_o + \delta} \right)^{2n} - 2 \left( \frac{r_o}{r_o + \delta} \right)^n \right\} \quad (1)$$

where  $\gamma$ ,  $r_o$ ,  $n$  and  $\delta$  are surface energy per unit area, scale parameter, shape parameter and crack opening displacement respectively. The surface energy  $\gamma$  which is required to form the new surface is a material constant. The values of the surface energy and the other parameters  $n$  and  $r_o$  are found experimentally. Thus the surface potential  $\phi$  is a continuous function of opening displacement  $\delta$ .

The derivative of interface potential  $\phi$  with respect to crack opening displacement  $\delta$  gives the bonding stress  $\sigma$  on the crack surface.

$$\sigma = \frac{\partial \phi}{\partial \delta} = \frac{4\gamma n}{r_o} \left\{ \left( \frac{r_o}{r_o + \delta} \right)^{n+1} - \left( \frac{r_o}{r_o + \delta} \right)^{2n+1} \right\} \quad (2)$$

Further, the bonding strength per unit area becomes a maximum under the following condition.

$$\frac{\delta}{r_o} = \left\{ \left( \frac{2n+1}{n+1} \right)^{\frac{1}{n}} \right\} - 1 \quad (3)$$

The maximum bonding strength  $\sigma_{cr}$  is given by,

$$\sigma_{cr} = \frac{4\gamma n}{r_o} \left\{ \left( \frac{n+1}{2n+1} \right)^{\frac{n+1}{n}} - \left( \frac{n+1}{2n+1} \right)^{\frac{2n+1}{n}} \right\} \quad (4)$$

To find the stress intensity factor,  $K$  from the crack opening displacement  $\delta$ , the following expressions can be used:

$$\delta = \left( \frac{8\sigma_y a}{\pi E} \right) \ln \sec \frac{\pi \sigma}{2\sigma_y} \quad (5)$$

When  $\sigma/\sigma_y \ll 1$

$$\delta = \frac{K^2}{\sigma_y E} \quad (6)$$

where  $a$  is crack length,  $\sigma$  is remotely applied stress and  $\sigma_y$  is the yield stress. To find crack-tip opening displacement any commercial FEM software can be used.

Further the stress intensity factor for a particular loading and crack conditions can be calculated by using the ANSYS code and in this study this approach has been adopted. As a condition of crack-tip extension (i.e. criterion of crack tip extension), the equation (4) is used in authors' written ANSYS code.

After evaluating the stress intensity factor  $K$ , the fatigue crack growth rate can be calculated using the Griffith-Irwin empirical equation [www.utm.edu] that fits the entire crack growth region.

$$\frac{da}{dN} = \frac{C(\Delta K - \Delta K_{th})^m}{(1-R)K_{crit} - \Delta K} \quad (7)$$

where  $R$  is the stress ratio, equal to  $\sigma_{min}/\sigma_{max}$ ,  $K_{crit}$  is critical stress intensity factor,  $m$  and  $C$  are material dependent constants,  $\Delta K_{th}$  is threshold stress intensity factor. The essential part of this equation (7) is to calculate the stress intensity factor range,  $\Delta K$ . Since there is no closed form solution of  $\Delta K$ , an empirical equation of the form  $\Delta K = \alpha \Delta \sigma \sqrt{\pi a}$  is usually assumed to relate the range of stress intensity factor, with the nominal stress range,  $\Delta \sigma$  and with the crack length,  $a$ ; and  $\alpha$  is a factor related to the specific geometry in question.

In order to appropriately assess fatigue crack propagation in welded joints it is necessary to obtain accurate results for stress intensity factor solution in the crack propagation phase. Generally the stress intensity factor for a crack in a welded joint depends on the global geometry of the joint, which include the weld profile, crack geometry, residual stress condition, the properties of HAZ (heat-affected-zone) material and the type of loading. Therefore, the calculation of the stress intensity factor, even for simple types of weldments, requires detailed analysis of several geometric parameters and loading systems. The two approaches that have mostly been used till now for assessing stress intensity factors for crack in weldments are weight function method [Bueckner (1970)] and the finite element method.

The FEM enables the analysis of complicated weld geometry due to its great versatility. It is able to use elastic-plastic elements to include crack tip plasticity. In FEM the stress intensity factor can be calculated directly from the stress field or from the displacement field around the crack tip. In this study FEM has been used for calculation of stress intensity factor.

After integrating the above expression, the fatigue crack

propagation life  $N_p$  is obtained by the following expression,

$$N_p = \int_{a_0}^{a_f} \frac{(1-R)K_{crit} - \Delta K}{C(\Delta K - \Delta K_{th})^m} da \quad (8)$$

The debonding model and the fracture mechanics crack growth model are essentially the same. The debonding model is used for the calculation of range of stress intensity factor  $\Delta K$  in equation (7) using the concept of debonding (equation (4)) and using equations (7) and (8) fatigue crack growth rate and propagation life is calculated. All other values in Equation (7) are known or assumed. This equation (7) is applicable for the entire three regions of the crack growth curve. Crack initiation growth rate or initiation life has not been modeled in this analysis. This model is being used for the calculation of crack propagation life, taken just after the range of the threshold stress intensity factor,  $\Delta K_{th}$ .

#### 4 Properties of Interface Elements

The interface elements employed in this study (Fig. 1) are the distributed nonlinear truss elements existing between two surfaces forming the crack surfaces. They are assumed to have zero mass and zero volume.

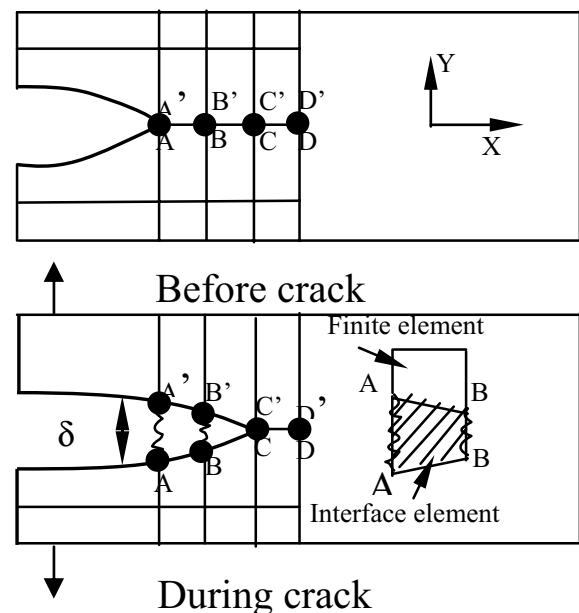
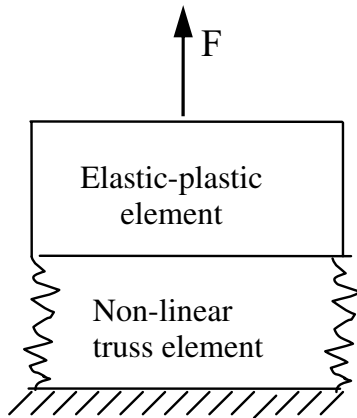


Figure 1 : Interface element between crack faces

Figure 2 represents a model of two linearly connected elements. The top element represents an elastic-plastic continuum, which represents the plastic zone near the crack tip. The non-linear truss element represents a potential failure surface.

The relation between the bonding stress ( $\sigma$ ) and crack opening displacement ( $\delta$ ) is shown in Fig. 3. When the opening displacement is small, the bonding between the two surfaces is maintained. As the opening displacement increases, the bonding stress increases until it reaches a maximum value  $\sigma_{cr}$ . With further increase in  $\delta$ , the bonding strength is rapidly lost and the surfaces are completely separated.



**Figure 2** : Interface element as a combination of non-linear truss and elastic-plastic elements

The mechanical properties of these two non-linear elements are characterized by the following sets of parameters,  $(\gamma, r_o)$  and  $(E, \sigma_y, h)$ , respectively. The parameter  $\gamma$  and  $r_o$  are the surface energy and the scale parameter of the interface.

The parameters  $E$ ,  $\sigma_y$ , and  $h$  are Young's modulus, the yield stress and the tangent modulus (slope of plastic portion of stress-strain curve) for a multilinear or bilinear material respectively. The mechanical behavior of the idealized elastic-plastic continuum can be represented by Fig.4.

## 5 Equilibrium Equation of the System

For simplicity, the outline of the mathematical formulation is presented for crack propagation in an elastic solid.

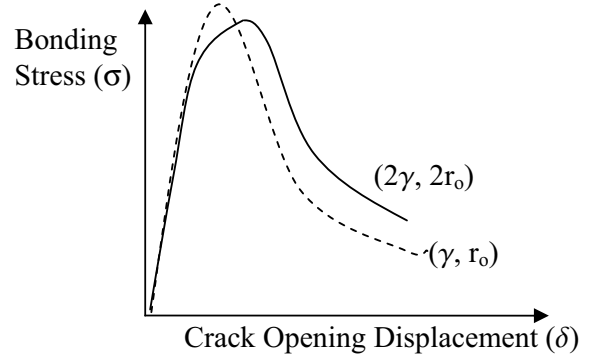


**Figure 3** : Mechanical properties of interface elements

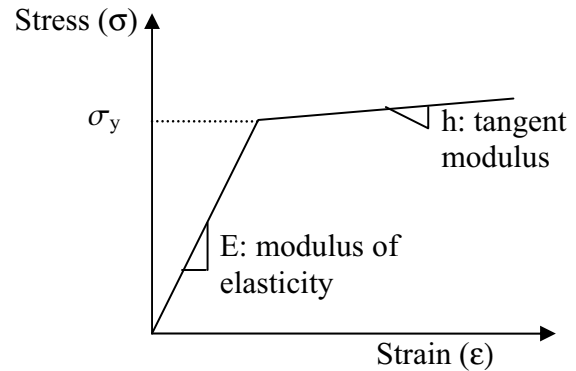


**Figure 4** : Mechanical properties of elastic-plastic continuum

When the material is elastic, the equilibrium equation can be derived based on the principle of minimum potential energy.

The total energy  $\Pi$  of the elastic body with a propagating crack can be described [Masakazu, Hisashi and Murakawa (2000)] as the sum of the strain energy  $U$ , the potential of external load  $W$  and the interface energy of the newly formed surface during crack propagation  $U_s$ , i.e.

$$\Pi = U + U_s + W \quad (9)$$

In the finite element method, the elastic body to be analyzed is subdivided into small elements and the displacements in each element are interpolated by nodal displacement  $u_o$ . The total energy is described as

$$\Pi = \Pi(u_o) = U(u_o) + U_s(u_o) + W(u_o) \quad (10)$$

Further,  $U(u_o), U_s(u_o), W(u_o)$  can be represented as the sum of the contributions from each element  $U^e(u_o^e), U_s^e(u_o^e), W(u_o^e)$ , i.e.

$$\Pi(U_o) = \Sigma\{U^e(u_o^e), U_s^e(u_o^e), W(u_o^e)\} \quad (11)$$

where  $u_o^e$  is the nodal displacement vector for each element extracted from the nodal displacement vector of the whole system  $u_o$ .

Once the total energy  $\Pi$  is given as in Eq. (11), the equilibrium equation in incremental form can be derived in the following manner. Denoting the nodal displacement at the present step and its increment to the next step as  $u_o$  and  $\Delta u_o$ , the total energy  $\Pi$  can be described as a function of  $u_o + \Delta u_o$  and can be expanded in a Taylor's series, i.e.

$$\begin{aligned} \Pi(u_o + \Delta u_o) &= \Pi(u_o) + \Delta^1 \Pi(\Delta u_o) + \Delta^2 \Pi(\Delta u_o) \\ &= \Pi(u_o) - \{\Delta u_o\}^T \{f\} + \frac{1}{2} \{\Delta u_o\}^T [K] \{\Delta u_o\} \end{aligned} \quad (12)$$

where  $\Delta^1 \Pi$  and  $\Delta^2 \Pi$  are the first and second terms in  $\Delta u_o$ , i.e.

$$\Delta^1 \Pi(\Delta u_o) = -\{\Delta u_o\}^T \{f\} \quad (13)$$

$$\Delta^2 \Pi(\Delta u_o) = \frac{1}{2} \{\Delta u_o\}^T [K] \{\Delta u_o\} \quad (14)$$

Further, the equilibrium equation can be derived as the stationary condition of  $\Pi(u_o + \Delta u_o)$  with respect to  $\Delta u_o$ ,

$$\partial \Pi(u_o + \Delta u_o) / \partial \Delta u_o = -\{f\} + [k] \{\Delta u_o\}$$

or

$$[k] \{\Delta u_o\} = \{f\} \quad (15)$$

where  $[k]$  and  $\{f\}$  are the tangent stiffness matrix and the load vector, respectively.

## 6 Stiffness Matrix and Force Vector of Interface Element

The stiffness matrix and the load vector of the interface element can be derived in basically the same manner as that for the whole system. The two surfaces separate when the load is applied. The opening displacement is denoted by  $\delta$  the surface area of the interface element is  $S^e$  and the interface energy for an element  $U_s^e(u_o^e)$  is given by the following equation [Murakawa and Zhengqi (1999)].

$$U_s^e(u_o^e) = \int \phi(\delta) dS^e \quad (16)$$

where  $\delta$  is the crack opening displacement at an arbitrary point on the surface that can be interpolated using an interpolation function  $N_i(\xi, \eta)$ , i.e.

$$\delta(\xi, \eta) = \Sigma N_i(\xi, \eta) (w_{i+4} - w_i) \quad (17)$$

where

$$N_1(\xi, \eta) = 0.25(1 + \xi)(1 - \eta),$$

$$N_2(\xi, \eta) = 0.25(1 + \xi)(1 + \eta),$$

$$N_3(\xi, \eta) = 0.25(1 - \xi)(1 + \eta),$$

$$N_4(\xi, \eta) = 0.25(1 - \xi)(1 - \eta)$$

and  $w_i$  is the nodal displacement normal to the surface. These interpolations are for a 3-D model where the interface elements are 2-D. But for a 2D model the interface element is 1-D and the shape functions are given by:

$$N_1(\xi) = 0.5\xi(\xi - 1), \quad N_2(\xi) = -(\xi + 1)(\xi - 1),$$

$$N_3(\xi) = 0.5\xi(\xi + 1)$$

Finally, the tangent stiffness matrix  $[k_e]$  and the load vector  $\{f^e\}$  of the interface element can be derived by expanding  $U_s^e(u_o^e + \Delta u_o^e)$  with respect to  $\Delta u_o^e$  in the following manner.

$$\begin{aligned}
 U_s^e(u_o^e + \Delta u_o^e) &= \int \phi(\delta + \Delta\delta) ds^e \\
 &= \int \phi(\delta) ds^e + \int \frac{d\phi(\delta)}{d\delta} \frac{\partial\delta}{\partial u_o^e} \Delta u_o^e ds^e \\
 &+ \frac{1}{2} \int \frac{d^2\phi(\delta)}{d\delta^2} \left(\frac{\partial\delta}{\partial u_o^e} \Delta u_o^e\right)^2 ds^e \\
 &+ \text{higher order terms}
 \end{aligned} \tag{18}$$

where

$$\int \frac{d\phi(\delta)}{d\delta} \frac{\partial\delta}{\partial u_o^e} \Delta u_o^e ds^e = -\{f^e\}^T \{\Delta u_o^e\} \tag{19}$$

and

$$\frac{1}{2} \int \frac{d^2\phi(\delta)}{d\delta^2} \left(\frac{\partial\delta}{\partial u_o^e} \Delta u_o^e\right)^2 ds^e = \frac{1}{2} \{\Delta u_o^e\}^T [k^e] \{\Delta u_o^e\} \tag{20}$$

Since the interface element has no volume or mass, the same formulation can be applied to both static and dynamic problems. By arranging the interface elements along the crack extension path in the simple model, crack propagation problems can be analyzed.

## 7 FEM Simulation of Fatigue Crack Growth

A new approach for crack propagation by killing or “death” elements (deactivate the element properties) is introduced in this analysis (birth and death option in Ansys 7.1). A bundle of non-linear truss elements as shown in Fig. 5, each having different material properties (modulus of elasticity, yield stress and tangent modulus) is used to connect to each boundary node ahead of the initial crack tip.

These values are lower to higher order from the crack tip to the other end. These elements have the same cross-sectional area and have capabilities to take both tension and compression loads. The stiffness of each truss element in terms of modulus of elasticity has different values from an extremely large value (210 GPa) (other end from the crack tip) to a value near the yield stress (280 MPa) (near crack tip). During each cycle of loading and unloading, the stiffness of each truss element is decreased by a certain amount (depends on total number of interface elements) using the MPCHG (ANSYS command to

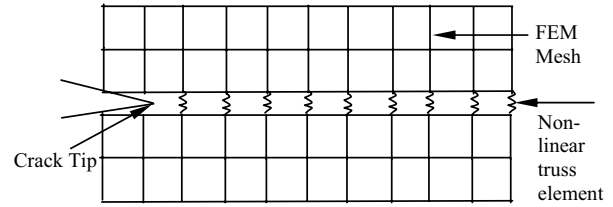


**Figure 5 :** A schematic views of the truss elements connected between two surfaces of separate mild steel plates having same material properties.

change properties) command. After each cycle of loading and unloading, the elemental axial stress is calculated. When any element’s stress exceeds the critical bonding stress that element is killed (deactivated material property) by using EKILL command. At the same time the element material properties from the crack tip to the other end is moved (changed) successively. Similarly, after ten cycles, the stress intensity factor at the crack tip (next to the killed element) is calculated by defining the crack path and using the KCALC command. From the stress intensity factor, the crack growth rate is calculated using equation (7) and the crack propagation life using equation (8).

This method has several advantages compared to other available numerical methods. The node release by killing elements can be performed at any time during a cyclic loading process irrespective of the magnitude of the deformation caused by the release of the nodes. Furthermore, several elements can be killed simultaneously, e.g. during a single overload cycle (which is higher than the yield strength of the material). This method overcomes the limitation of crack propagation of one element length during each cycle of loading. In this method, the crack propagates automatically when the element’s stress exceeds the bonding stress of the element. Here a crack can propagate in more than one direction but a limitation is that the possible directions have to be determined earlier depending on the physical crack configuration, loading and material homogeneity. For bi-axial (multi load) loading where the crack directions are not obvious, this method may be suitable.

### 7.1 Overall Methodology for Fatigue Life Calculation

The critical stress intensity factor for short-term fracture  $K_{crit}$ , material constants  $C$  and  $m$ , and the threshold stress

intensity factor range  $\Delta K_{th}(R)$  as a function of  $R$  for the material to be analyzed is determined or collected from literature ( $\Delta K_{th}(R)$  as a function of  $R$  could be found [Anderson (1994)]).

The values of the surface energy per area  $\gamma$ , the scale parameter  $r_o$ , and the shape parameter,  $n$  for the material are determined experimentally or collected from literature.

The Finite Element model is created and the interface elements are introduced in the possible crack propagation directions (maximum stress concentration, weld defect, etc). The critical bonding stress,  $\sigma_{cr}$  of the interface elements is determined using the equation (4). The plastic zone radius is calculated using the standard equation and the elastic-plastic material properties are applied to the elements within the plastic zone.

The cyclic load for a particular stress ratio is applied to the model and after each cycle of loading the interface element-stress is calculated. When any element stress exceeds the critical bonding strength, (which was calculated using equation (4)), that element is killed. Thus after some cycles (10 to 20 cycles or more) the crack propagation is viewed (only the active elements are viewed and killed elements are kept hidden) and the final crack length is determined. For the same crack length and stress conditions, the stress intensity factor is calculated using Authors' ANSYS input files. All the works in steps 3 and 4 of this section are computed using authors' written ANSYS input files. In written code, equation (4) is used as a condition of crack extension which affect the crack-tip region and eventual calculations of stress intensity factor. The crack tip front region is simulated using interface element and its properties. The crack will only propagate when the interface "element-stress" near the crack tip exceeds the critical bonding stress calculated using equation (4). Furthermore, the displacement field around the crack tip is influenced by the properties of the interface elements (since the crack tip front region is simulated using interface element and its properties), and consequently, the stress intensity factor will also be influenced by interface elements' properties. The material properties of the interface elements are changed after each cycle.

The fatigue crack growth rate and the fatigue life are calculated using equation (7) and (8).

## 8 Case Studies

Two cases are considered here: Case (a) A 2-D finite element model of a curve T-joint (600 x 15 x 10 mm (web) 400 x 75 x 10 mm flange) (Fig 6a) and Case (b) A 3-D finite element model of a curve plate (381 x 15x 4mm, radius of curvature 1041.4 mm) (Fig 6b) are created and interface elements as described above are applied in the crack faces. In curve plate, the applied stress produces moment, which can not be represented in 2-D model. Therefore a 3-D model is created and shells 181 elements which have bending capacity is used in the model.

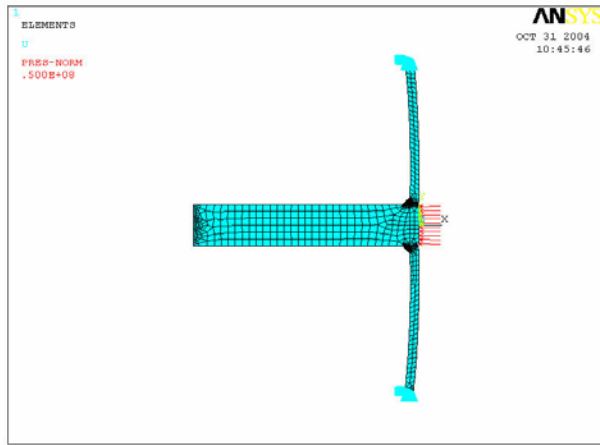
The curve T-joint represents the connection of shell plate with transverse girder of ship/aircraft structures. This joint experiences fluctuating wave load in the case of ship. The top and bottom side of both models are fixed in all degrees of freedom and a cyclic load is applied at the right side. The amplitudes of cyclic loads (minimum 10 MPa, maximum 200 MPa) shown in Fig. 7 are applied to the model. The model is created and analyzed by writing ANSYS input files as mentioned in Section 7.

The mechanical properties of base, weld and heat-affected-zone (HAZ) materials as shown in Table 1 are applied to the model. The Paris' crack growth rate constants for steel are assumed as:  $C = 3 \times 10^{-11}$ ,  $m = 4$ . The  $\Delta K_{th}$  values were taken as 4, 5, 6 MN/m<sup>3/2</sup> for stress ratios of 0.3, 0.2 and 0.1 respectively, from Fig.10.9 in [Anderson (1994)] for this particular weld. The critical stress intensity factor  $K_{crit}$  is taken as 150 MN/m<sup>3/2</sup> which is an average value of the critical stress intensity factor for mild steel. The value of the critical stress intensity factor for mild steel are reported to be in the range from 100 to 200 MN/m<sup>3/2</sup>. Therefore, it is reasonable to take an average value of 150 MN/m<sup>3/2</sup>. In addition, the residual stresses of different magnitudes at different weld regions are applied. The residual stress values varied from 120 MPa (tension) to -120 MPa (compression) from the center to the edge of weld as found in [Glinka(1994)]. It is assumed that for this welded joint the crack initiation phase is very short and insignificant due to the presence of initial welding defects. Initial crack length has been assumed to be 4 mm. An axial cyclic load near the yield strength of the material is applied for various cycles, and the corresponding stress intensity factor and crack opening displacement are calculated from the FEM analysis. Then using equation (7) and (8), the fatigue crack growth rate and fatigue crack propagation life are calculated.



**Table 1** : Mechanical properties of base, weld and heat-affected-zone materials [Burk (1978)]

Material	Modulus of elasticity, E (GPa)	0.2% offset Yield strength (MPa)	Ultimate tensile strength (MPa)
ASTM A36	190	224	414
Weld material E60S-3	189	580	710
A36 HAZ	189	534	667



(a)

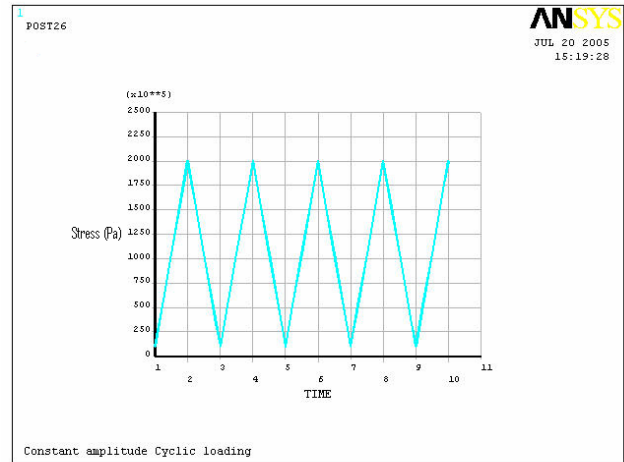
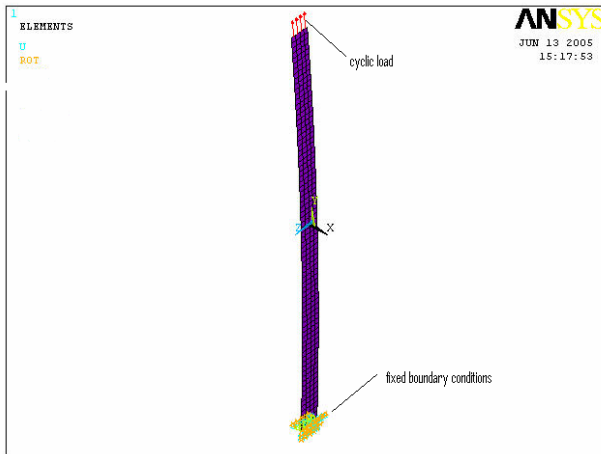


**Figure 7** : A typical constant amplitude axial cyclic load



(b)

**Figure 6** : (a) A 3-D FEM model of welded curve T-joint (600 x 15 x 10 mm (web) 400 x 75 x 10 mm flange); (b) A 2-D FEM model of welded curve plate (381 x 15 x 4mm, radius of curvature 1041.4 mm).

**9 Results and Discussions**

For case (a), the fatigue crack growth rates for different stress ratios, R are calculated and shown in Fig. 8. As

the stress ratio decreases, the crack growth rate increases. When the stress ratio increases, the range of stress increases and hence the crack growth rate increases. Again, generally the range of threshold stress intensity factor decreases with increase of stress ratio. The threshold stress intensity factor is a function of stress ratio ( $\Delta K_{th} = K_{op}(1 - R)$ ), where  $K_{th}$  is threshold stress intensity factor,  $K_{op}$  is crack opening stress intensity factor and R is the stress ratio). According to equation (7), the crack growth rate decreases with increases of  $\Delta K_{th}$ . The results of Fig. 8 shows this trend and gives a good indication of the effectiveness of this method. Further, the difference in crack growth rate for different stress ratios at high range of stress intensity factor is smaller than that at low range of stress intensity factor. This may be due to the effect of threshold stress intensity factor. At low stress level i.e. low range of stress intensity factor; the effect of threshold stress intensity factor over crack growth rate is more than at high stress level. Furthermore, after the range of stress intensity value about 8, the crack growth rate becomes constant for all stress ratios. This may also be for threshold stress intensity factor. For this type of mild steel, the threshold stress intensity factor is less than  $8 \text{ MN/m}^{3/2}$ .

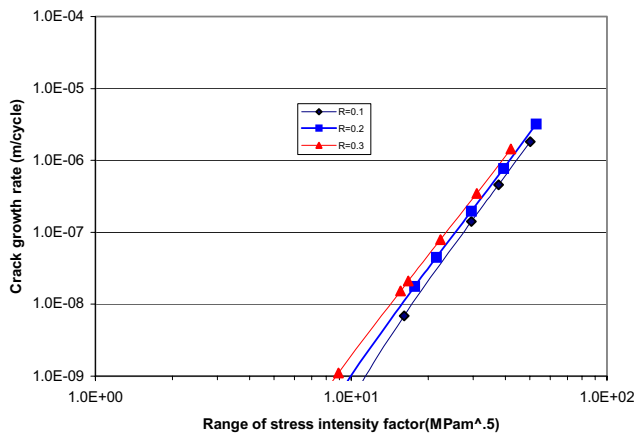


**Figure 8 :** Fatigue crack growth rate with the range of stress intensity factor (for case a).

Therefore, there is less effect of threshold stress intensity factor on fatigue crack growth rate after  $8 \text{ MN/m}^{3/2}$ .

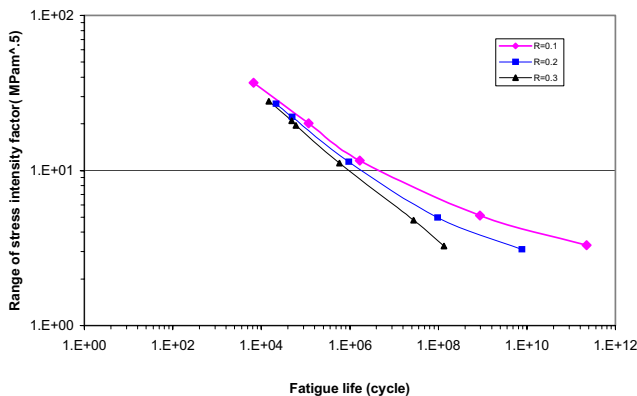


**Figure 9 :** Variation of fatigue life with range of stress intensity factor (for case a)

The variation of fatigue life with range of stress intensity factor for three stress ratios is shown in Fig.9. The fatigue life increases at low stress intensity factor and the trend is to become infinity below threshold stress intensity factor. Because at low stress level, the accumulation of fatigue crack growth is very low and the fatigue life increases toward infinity. On the other hand, the fatigue life decreases with the increase of stress intensity factor. For a particular range of stress intensity factor 10, the fatigue life decreases about 20 % at stress ratio 0.2 and 38 % at stress ratio 0.3 comparing to that at stress ratio 0.1.

The variation of crack opening displacement with crack tip stress is shown in Fig. 10. The crack opening displacement (COD) increases with crack tip stress.

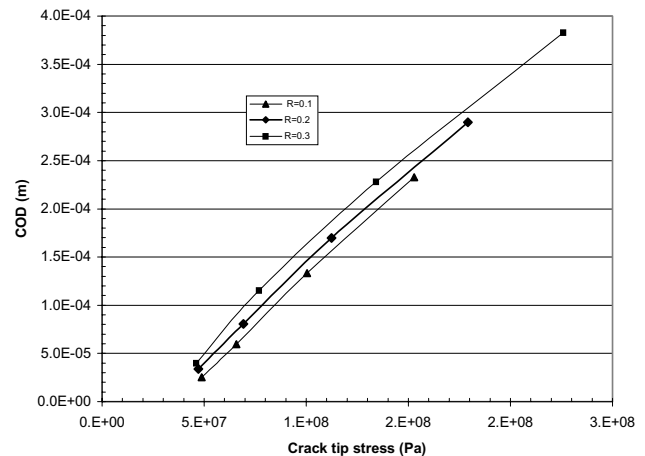


**Figure 10 :** Variation of crack tip opening displacement (COD) with crack tip stress (for case a)

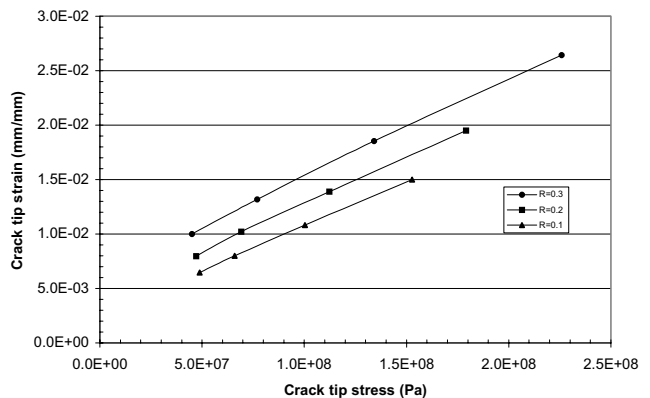


**Figure 11 :** Variation of strain at crack tip with crack tip stress (for case a)

placement (COD) increases with crack tip stress. For a particular crack tip stress, the COD increase with increases of stress ratios. In this case, load amplitude was constant; increasing both minimum and maximum load has changed the stress ratios. Therefore, the stress ratio increases with the increases of maximum stress. The results shown here are for the maximum load only. For this reason, the COD increases with the increase of stress ratio. Further at low stress, the variation of COD is less (0.03 mm) comparing to high stress level (0.15 mm). The crack tip stress increases with the increases of crack length. So the COD increases with the increases of crack tip stress.

The variation of strain in the y-direction at the crack tip with crack tip stress is shown in Fig. 11. The strain in-

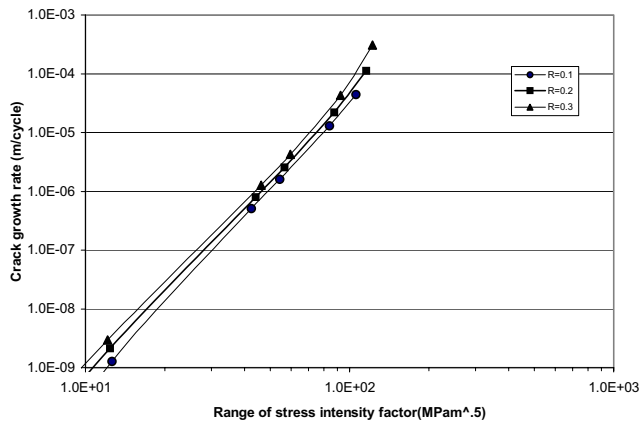


**Figure 12 :** Fatigue crack growth rate with the range of stress intensity factor (for case b).

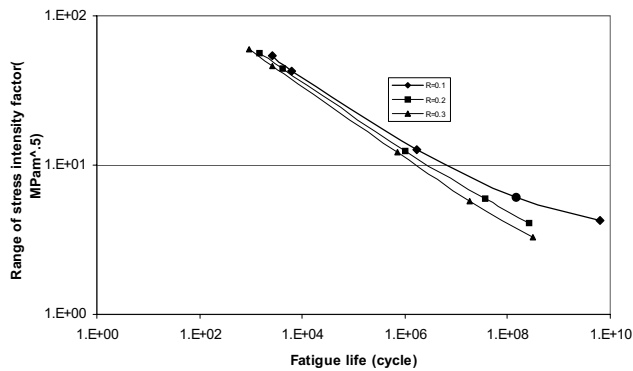


**Figure 13 :** Variation of fatigue life with range of stress intensity factor (case b)

creases with crack tip stress. At low crack tip stress, the change in strain for different stress ratios is less comparing to that in high crack tip stress. The crack tip stress increases with increases of crack length. As the crack length increases, the material stiffness decreases and crack tip stress increases, and hence the strain increases.

For case (b), the fatigue crack growth rate for different stress ratios, R is shown in fig. 12. For case (b), the crack growth rate is higher than that in case (a). Because in case (b), the bending effect may accelerates the crack growth rate.

The crack growth rate increases rapidly above the starting point of the fast fracture. At the fast fracture, the material losses stiffness and stability and the crack growth rate increases rapidly.

The variation of fatigue life with range of stress intensity

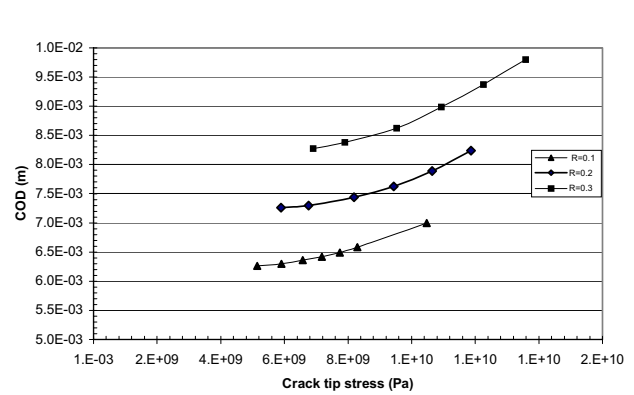


**Figure 14 :** Variation of crack tip opening displacement (COD) with crack tip stress (case b)

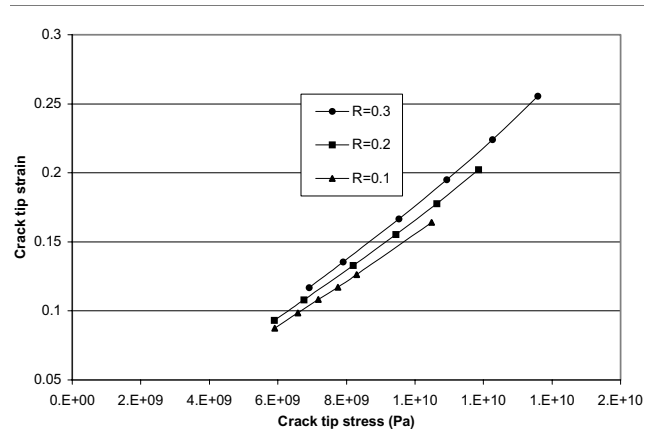


**Figure 15 :** Variation of strain at crack tip with crack tip stress (case b)

factor for case (b) is shown in Fig.13. For the same reason i.e. the bending effect, in case (a) the fatigue crack growth rate is less comparing to that in case (b). Therefore the fatigue life increases in case (a) comparing to case (b). At low range of stress intensity factor the fatigue life increases rapidly and its trend is toward infinity. At low stress level, the accumulation of fatigue crack growth is very low (1E-9 m/cycle) and the fatigue life increases toward infinity.

The variation of crack opening displacement with crack tip stress for case (b) is shown in Fig. 14. The crack opening displacement (COD) increases with the increases of crack tip stress. Since in case (b), the bending stress accelerates the crack growth, the COD in case (a) decreases comparing to that in case (b).

The variation of strain at the crack tip with crack tip stress

for case (b) is shown in Fig. 15. The strain increases with crack tip stress. At low crack tip stress, the change in strain for different stress ratios is less comparing to that in high crack tip stress. The crack tip stress increases with increases of crack length. As the crack length increases, the material stiffness decreases and hence the strain increases. Further for similar reason, the strain in case (a) decreases comparing to that in case (b).

### 9.1 Traditional FEM Model for Fatigue Crack Propagation

Traditional FEM model for an edge-cracked plate is shown Fig. 16. In the lower edge of the plate symmetric boundary condition is applied and in the upper edge cyclic stress loading is applied. In traditional FEM, the crack tip is extended one element length per cycle when the applied stress reached the maximum level. For each increment of the crack extension, a stress analysis is carried out and the stress intensity factors are evaluated. Similarly in this traditional model one crack tip node (from left side) is released (degrees of freedom is deleted or stiffness is set zero) after each cycle and stress intensity factor is calculated.

The comparison of fatigue crack propagation life between new (Interface Model) and traditional FEM model is shown in Fig. 17. It is found that in the traditional method, the fatigue crack propagation life is less comparing to that in the new proposed method. Since for the same stress level the displacement field around the crack tip is influenced by the properties of the interface element near the crack tip, the stress intensity factor has been changed due to interface elements' properties. Further, the final crack lengths are also found different in this method for the same cycle of applied load. Furthermore, the difference in fatigue life at low stress range is more than in the high stress range, because at higher stress cycles, crack initiation occurs much faster.

### 9.2 Comparison with Experimental Results

For validation, the predictions have been compared with the experimental results obtained using universal MTS testing machine for curve plates. The experimental results are for a single-V butt welded curve plate joint of the dimensions (381 x 15 x 4 mm) as shown in Figure 18. The mechanical properties of the weld material are the same as shown in Table 1. Similar model (same geometric and mechanical properties) has been analyzed using

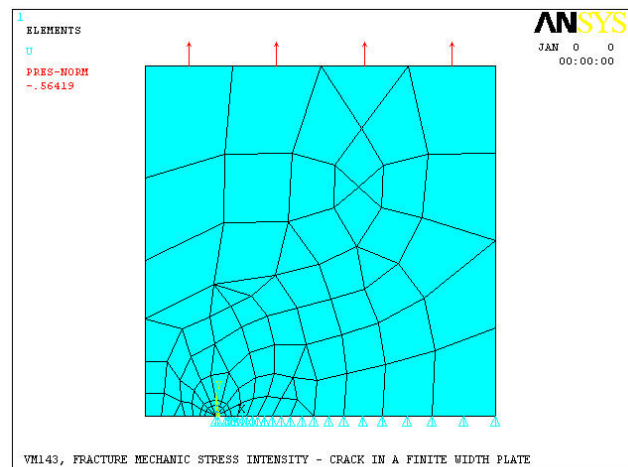


Figure 16 : Traditional FEM model for fatigue crack propagation

the authors' computer program and ANSYS code. The stress ratios for both the cases (experimental and prediction) are the same ( $R=0$ ) and the maximum loads are also the same (150, 180, 200, 220, 250 MPa respectively). The initial crack lengths for both the cases are considered to be 4 mm. The comparison is shown in Fig 19. At low and high stress range, the trend of both the results is different but at medium stress range, the difference is low. At  $2 \times 10^6$  cycles, the percentage change in the stress range is about 6.

This difference may be due to a different threshold stress intensity factor. The threshold stress intensity factor used in this analysis is collected from the literature [Anderson (1994)] available in the field and an average value dependent on stress ratio was assigned. In the experiment, threshold stress intensity factor need not to be considered separately and it is counted automatically. Another reason for this slight deviation may be the effect of residual stress. The residual stresses used in the prediction model are in the range from  $-120$  MPa to  $120$  MPa but in the experiment these values may be slightly different. Further during welding of curve plate, the radius of curvature may be changed. Furthermore the mechanical properties also might be slight different from values collected from literature.

## 10 Conclusions

The proposed simulation of fatigue crack propagation using an interface element is simple in formulation, ef-

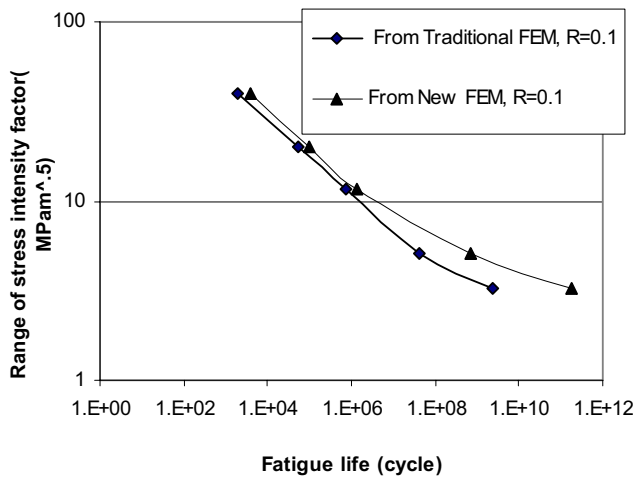


**Figure 17 :** Comparison of fatigue crack propagation life from new and traditional FEM model for center crack plate

fective in practice, and numerically less intensive. This method can be applied in T- and curve plate butt-joints. The method can be applied for symmetric and anti-symmetric planes under cyclic load and also for bending loading. This method overcomes the limitation of crack tip extension at a rate of one element length per cycle. In this method the crack propagates only when the applied load reaches the critical bonding strength.

**Acknowledgement:** The authors wish to acknowledge the support received from the Louisiana State Economic Development Grant and Louisiana Board of Regent's LaSpace Consortium Project # 127404104 and Louisiana State University Mechanical Engineering Department for providing the facilities for this research.

## References

- Alam M.S. and Wahab M.A.** (2005): Modeling of Fatigue Crack Growth and Propagation Life of Joint of Two Elastic Materials Using Interface Elements, *International Journal of Pressure Vessel and Piping*, **82**, pp. 105-113.
- Anderson T.L.** (1994): *Fracture Mechanics, Fundamentals and applications*, 2nd edition, CRC press, Boston, USA.
- Bueckner H.F.** (1970): A novel principle for the computation of stress intensity factors, *Zeitschrift Angewandte Mathematik and Mechanik*, **50**, pp. 129-146.

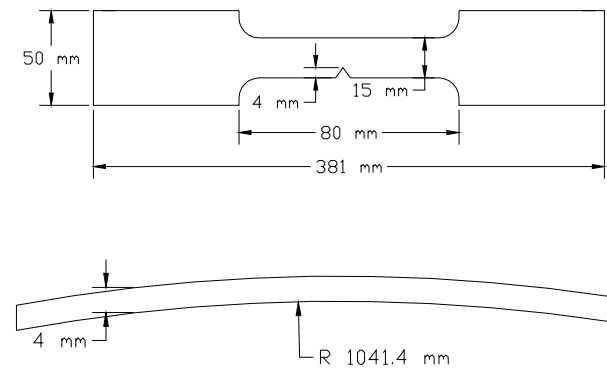


**Figure 18 :** Specimen size of curve plate

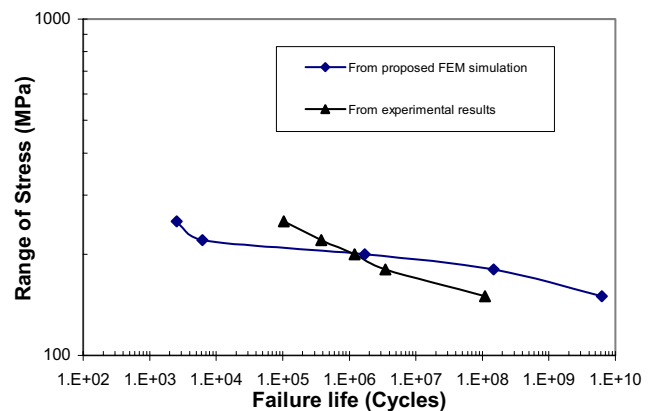


**Figure 19 :** Comparison of prediction and experimental results

**Burk J. D.** (1978): *Fatigue crack initiation and propagation life estimates*, Ph.D thesis, Department of Metallurgy and Mining, University of Illinois, Urbana-Champaign, Illinois, USA.

**Chermahini R.G., Shivakumar K.N. and Newman J.C.** (1988): Three dimensional finite element simulations of fatigue crack growth and closure, *ASTM STP 982*, Philadelphia, PA, pp. 398-401.

**Masakazu S., Hisashi S. and Murakawa H.** (2000): Finite element method for hot cracking using temperature dependent interface element (report II), *Journal of Welding Research Institute*, **29** (1), pp. 59-64.

**McClung R.C. and Sehitoglu H.** (1989): On the finite element analysis of fatigue crack closure-I, basic modeling issue, *Journal of Engineering Fracture Mechanics*, **3**, pp. 237-252.

**Murakawa, M., Hisashi S. and Zhengqi W.** (2000): Strength analysis of joints between dissimilar materials using interface elements, *Journal of Welding Research Institute*, **29(2)**, pp. 71-75.

**Murakawa H. and Zhengqi W.** (1999): Computer simulation method for crack growth using interface element employing Lennard Jones type potential function, *Material Science Research International*, **5(3)**, pp. 195-201.

**Newman J.C., and Harry A. J.** (1975): Elastic-plastic analysis of a propagating crack under cyclic loading, *Journal of AIAA*, **13**, pp. 1017-2023.

**Newman J.C.** (1977): Finite-element analysis of crack growth under monotonic and cyclic loading, *ASTM STP 637*, Philadelphia, PA, pp. 56-80.

**The University of Tennessee at Martin :**  
[http://www.utm.edu/departments/engin\\_lemaster/Machine%20Design/Lecture%2012.pdf](http://www.utm.edu/departments/engin_lemaster/Machine%20Design/Lecture%2012.pdf)

**Wu J. and Ellyin F.** (1996): A study of fatigue crack closure by elastic-plastic finite element analysis for constant-amplitude loading, *International Journal of Fracture*, **82**, pp. 43-65.